Weak Ergodicity Breaking and Quantum Many-Body Scars in Spin-1 *XY* Magnets

Michael Schecter[1] and Thomas Iadecola[1,2]

[1]*Condensed Matter Theory Center and Joint Quantum Institute, Department of Physics, University of Maryland, College Park, Maryland 20742, USA*

[2]*Department of Physics and Astronomy, Iowa State University, Ames, Iowa 50011, USA*

(Received 1 July 2019; published 1 October 2019)

We study the spin-1 *XY* model on a hypercubic lattice in *d* dimensions and show that this well-known nonintegrable model hosts an *extensive* set of anomalous finite-energy-density eigenstates with remarkable properties. Namely, they exhibit subextensive entanglement entropy and spatiotemporal long-range order, both believed to be impossible in typical highly excited eigenstates of nonintegrable quantum many-body systems. While generic initial states are expected to thermalize, we show analytically that the eigenstates we construct lead to weak ergodicity breaking in the form of persistent oscillations of local observables following certain quantum quenches—in other words, these eigenstates provide an archetypal example of so-called quantum many-body scars. This Letter opens the door to the analytical study of the microscopic origin, dynamical signatures, and stability of such phenomena.

DOI: 10.1103/PhysRevLett.123.147201

Introduction.—Quantum ergodicity is a fundamental concept explaining how unitary quantum evolution can lead to an equilibrium state described by statistical mechanics. While the eigenstate thermalization hypothesis (ETH) [1–4] posits that *generic* closed quantum many-body systems exhibit ergodicity, there are important exceptions to this paradigm, including many-body localized systems [5], integrable systems [6] (which are nongeneric), dipole-conserving theories [7–9], and a relatively new class of weakly nonergodic systems exhibiting quantum many-body scars (QMBS) [10–19].

Ergodicity breaking in such systems can often be attributed to the presence of symmetries (hidden, emergent, or explicit) that preclude the establishment of a global equilibrium state. A notable exception arises in systems with QMBS, which exhibit nonergodic dynamics in the form of coherent oscillations of local observables after a quantum quench from certain initial states, as observed in a recent experiment in a Rydberg-atom quantum simulator [20]. In this case, the observed nonergodicity stems from the existence of an extensive set of special "scarred" eigenstates that are unrelated to any symmetry of the Hamiltonian [11]. This is a remarkable departure from the ETH scenario, wherein the finite-energy-density initial state would rapidly thermalize and lose coherence. The violation of ergodicity via scarring therefore presents a fundamental puzzle in our understanding of highly excited states in thermalizing systems that has spurred substantial recent interest.

The ubiquity and stability of QMBS are under active investigation. Multiple possible explanations of the underlying mechanism have been debated for the so-called PXP model realized in the Rydberg experiment [11,12,14–17,19,21–23], ranging from proximity to integrability [15], "embedded" SU(2) dynamics [14,24], and magnon condensation [19]; moreover, connections have been made to gauge theory [25], symmetry-protected topological phases [16,21], and quantum Hall physics [23]. Given these various perspectives, it is highly desirable to find a tractable realization of scarring that can be established rigorously and its nonergodic properties studied analytically. While exact scarred eigenstates of the Affleck-Kennedy-Lieb-Tasaki (AKLT) spin chains [26] have been constructed analytically [10,13], it is unclear whether and how these states lead to dynamical signatures resembling the experimental observations [20].

In this Letter, we study the spin-1 *XY* model on a hypercubic lattice in *d* dimensions. We show that this well-known model surprisingly harbors an extensive set of anomalous scarred eigenstates at finite energy density that exhibit subextensive entanglement entropy and long-range space-time crystalline order [27–29]. These scarred states survive certain continuous deformations of the model and are eigenstates of an emergent SU(2) algebra that is *not* part of the Hamiltonian's symmetry group. We further show that the scarred states lead to persistent oscillations of local observables following suitable quantum quenches. In particular, we show that quantum evolution starting from a suitable initial product state, prepared by applying a large symmetry-breaking field, shows perfect periodic revivals, while generic initial states rapidly thermalize. Our results thus firmly establish the existence of QMBS in the spin-1 *XY* model.

Model.—We study the spin-1 *XY* model

$$H = J\sum_{\langle ij\rangle}(S_i^x S_j^x + S_i^y S_j^y) + h\sum_i S_i^z + D\sum_i (S_i^z)^2, \quad (1)$$

where S_i^α ($\alpha = x, y, z$) are spin-1 operators residing on the sites i of a d-dimensional hypercubic lattice with volume $V = L^d$, and $\langle ij \rangle$ denotes nearest neighbors. We hereafter set $J = 1$ and assume either periodic or open boundary conditions (PBCs or OBCs) as noted. The scarred states we present here exist for both OBCs and PBCs and for any d, D, h. In the Supplemental Material [30], we present a class of spin-S generalizations of Eq. (1) that also exhibit QMBS.

H possesses a global U(1) symmetry generated by spin rotations about the z axis and, depending on boundary conditions, may have translation and/or point-group symmetries. For $d = 1$ and OBCs, H also has a nonlocal SU(2) symmetry [31], although this symmetry is not requisite for scarring and can be removed, e.g., by adding $H_3 = J_3 \sum_i (S_i^x S_{i+3}^x + S_i^y S_{i+3}^y)$. In fact, any U(1)-symmetric exchange term preserving the bipartite structure of the hypercubic lattice is allowed [30].

The Hamiltonian H is nonintegrable and, as we show in Fig. 1, the statistics of its many-body energy level spacings s in a symmetry sector with sufficiently many levels follows the Wigner-Dyson (WD) distribution. WD level statistics is a common proxy for chaotic and ergodic behavior in quantum systems and indicates the absence of hidden or emergent symmetries that would strongly influence the level statistics (e.g., integrable systems follow the Poisson distribution shown for comparison in Fig. 1).

It is well known that WD level statistics alone is not sufficient to guarantee that the *strong* ETH, positing that *all* states in an energy window obey the ETH [4], holds. In special cases, a weak form of the ETH may hold [33] that allows for a rare set of anomalous eigenstates that violate the ETH. This possibility is remarkable in light of the fact that there is no protecting symmetry that prevents the anomalous states from mixing with thermal states at the same energy. Nevertheless, we now demonstrate that this scenario holds for the spin-1 XY model (1). The strong

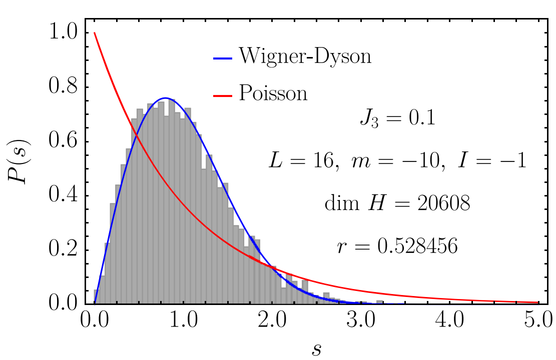

FIG. 1. Distribution of many-body level spacings s in the middle half of the spectrum of H for $d = 1$ with open boundary conditions and $J_3 = 0.1$, $D = 0$. The data are taken in the U(1) sector $\sum_i S_i^z = m = -10$ and the inversion sector $I = -1$. The r value [32] of the distribution given in the figure is close to the Wigner-Dyson result, $r_{\rm WD} \approx 0.5295$.

ETH fails due to the presence of the following athermal eigenstates:

$$|\mathcal{S}_n\rangle = \mathcal{N}(n)(J^+)^n|\Omega\rangle, \tag{2}$$

where $n = 0, \ldots, V$ is an integer, $|\Omega\rangle = \bigotimes_i |m_i = -1\rangle$ is the fully polarized "down" state, $m_i = -1, 0, 1$ are the eigenvalues of S_i^z, $\mathcal{N}(n) = \sqrt{(V-n)!/n!V!}$ are normalization factors, and

$$J^\pm = \frac{1}{2}\sum_i e^{i\boldsymbol{r}_i\cdot\boldsymbol{\pi}}(S_i^\pm)^2. \tag{3}$$

In Eq. (3), $\boldsymbol{r}_i$ are the spins' coordinates and $\boldsymbol{\pi} = (\pi, \pi, \ldots, \pi)$. The state $|\mathcal{S}_n\rangle$ contains n bimagnons (i.e., doubly raised spins), each with momentum $\boldsymbol{k} = \boldsymbol{\pi}$. In the Supplemental Material [30], we show that they are frustration-free eigenstates of the Hamiltonian (1) with energy $E_n = h(2n - V) + VD$ and total magnetization $m_n = 2n - V$. There we also highlight another (orthogonal) tower of exact eigenstates that arise for PBCs and $D = 0$ in $d = 1$.

Interestingly, the operators $J^\pm$ are generators of an SU(2) algebra (distinct from that of Ref. [31]) defined by

$$J^z = \frac{1}{2}\sum_i S_i^z; \quad [J^+, J^-] = 2J^z; \quad [J^z, J^\pm] = \pm J^\pm. \tag{4}$$

Note that the spin-1 nature of the microscopic spins is crucial for this algebra to hold. These SU(2) generators do not all commute with H: $[H, J^\pm] \neq 0$, while $[H, J^z] = 0$. Nevertheless, the scarred states (2) form a representation of this emergent SU(2) algebra with spin $j = V/2$ (the maximum possible value):

$$\boldsymbol{J}\cdot\boldsymbol{J}|\mathcal{S}_n\rangle = \frac{V}{2}\left(\frac{V}{2}+1\right)|\mathcal{S}_n\rangle, \tag{5}$$

where $\boldsymbol{J}\cdot\boldsymbol{J} = \frac{1}{2}(J^+J^- + J^-J^+) + (J^z)^2$. $J^\pm$ thus act as ladder operators for the scarred states:

$$J^\pm|\mathcal{S}_n\rangle = \sqrt{j(j+1) - \frac{m_n}{2}\left(\frac{m_n}{2} \pm 1\right)}|\mathcal{S}_{n\pm1}\rangle, \tag{6}$$

where $j = V/2$ and $m_n/2 = n - V/2$.

The scarred states (2) at generic n are not thermal even though they have finite energy density and reside in symmetry sectors with exponentially many states; hence, they violate ETH. To show this, we first consider their bipartite entanglement entropy $S_A = -{\rm tr}\rho_A \ln \rho_A$, where ρ_A is the reduced density matrix for a region A of size $V_A = V/2$. We plot S_A vs energy E for eigenstates in the zero-magnetization sector in Fig. 2, highlighting the lightly entangled scarred state $|\mathcal{S}_{V/2}\rangle$ with a red circle (eigenstates are obtained using exact diagonalization for

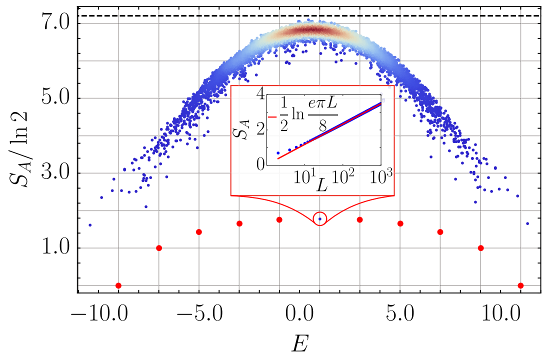

FIG. 2. Bipartite entanglement entropy S_A of eigenstates of H for $d=1$, $L=10$, and $(h,D,J_3)=(1,0.1,0.1)$ with OBCs. States in the zero-magnetization sector (smaller points) are color coded by the density of states (warmer colors imply higher density). The total number of states in this sector is $\dim H_{m=0}=8953$. The dashed line at $S_A^{\mathrm{ran}}=(L/2)\ln 3-\frac{1}{2}$ indicates S_A for a random state. Larger red points indicate scarred states (2) in U(1) sectors with $m_n\neq 0$. (Inset) S_A for $|\mathcal{S}_{L/2}\rangle$ as a function of L, cf. Eq. (7).

$d=1$, $L=10$). ETH-obeying states have extensive "volume-law" entanglement entropy, $S_A\propto V$. For states near the middle of the spectrum (nominally at infinite temperature), S_A should approach the value for a random state, $S_A^{\mathrm{ran}}=(V/2)\ln 3-\frac{1}{2}$ [34] (dashed line in Fig. 2), which appears to be approximately true for a large fraction of states near $E\approx 0$. Thus, to show that the states (2) violate the ETH, we need only show that their entanglement entropy is subextensive.

The simplicity of the states (2) allows for an analytical calculation of the full entanglement spectrum from which the entanglement entropy can be obtained (see the Supplemental Material [30]). The resulting values of S_A for the state $|\mathcal{S}_{V/2}\rangle$ are plotted in the inset of Fig. 2 as a function of system length L for $d=1$. In fact, one can show analytically that S_A takes the asymptotic form [30]

$$S_A(n=V/2)\underset{V\to\infty}{\longrightarrow}\frac{1}{2}\left(\ln\frac{\pi V}{8}+1\right), \tag{7}$$

cf. inset to Fig. 2. The state $|\mathcal{S}_{V/2}\rangle$ has the highest entanglement of all scarred states (2) (cf. Fig. 2), so Eq. (7) demonstrates conclusively that these states exhibit subextensive entanglement entropy scaling at most logarithmically with system size.

It is instructive to compare the scarred states (2) with other examples of exact excited states of nonintegrable models, in particular, the "η-pairing" states of the Hubbard model [35] and the scarred states of the AKLT chain [10]. Both of the latter examples also host towers of states with logarithmic entanglement [13,36] obtained by acting repeatedly with some operator on a parent state. The η-pairing example is unique in that it is protected by "η symmetry"; i.e., the analogs of $J^\pm$ are eigenoperators of the Hamiltonian and the η-pairing states are the only states in their respective symmetry sectors. Thus, the η-pairing states are neither ETH-violating nor bona fide scarred states (despite many similar features). The AKLT scarred states *do* violate the ETH and, interestingly, are created by the same operator J^+ as in Eqs. (2) and (3). However, the parent state in that case is the AKLT ground state rather than the fully polarized state $|\Omega\rangle$. This is crucial because the AKLT scarred states *do not* form a representation of the SU(2) algebra (4). It is an important outstanding question whether such a structure exists for the AKLT model, as it could be used to determine the dynamical signatures of the scarred states, which (to the best of our knowledge) remain unknown. For the scarred states presented here, this is not the case, and we now show that their dynamical signatures can be deduced directly from the SU(2) algebra (4).

Space-time crystalline order.—We first demonstrate the presence of off-diagonal long-range order (ODLRO) [37] in the scarred states associated with the condensation of bimagnons at momentum $\boldsymbol{\pi}$. Such order is also present in the η-pairing states, where it is indicative of superconductivity [35]. Here, the order is of a *spin-nematic* nature: the order parameter $O_{\boldsymbol{q}}=(1/V)\sum_i e^{i\boldsymbol{r}_i\cdot\boldsymbol{q}}(S_i^+)^2$ has long-range connected correlations at wave vector $\boldsymbol{q}=\boldsymbol{\pi}$ in the scarred states. This is indicated by a finite value of the correlation function $\langle\mathcal{S}_n|O_{\boldsymbol{\pi}}^\dagger O_{\boldsymbol{\pi}}|\mathcal{S}_n\rangle$ [note $\langle\mathcal{S}_n|O_{\boldsymbol{\pi}}^\dagger|\mathcal{S}_n\rangle=0$ by U(1) symmetry]. Using Eqs. (3) and (6), one immediately obtains

$$\langle\mathcal{S}_n|O_{\boldsymbol{\pi}}^\dagger O_{\boldsymbol{\pi}}|\mathcal{S}_n\rangle=1-m_n'^2+\mathcal{O}(1/V), \tag{8}$$

where the $\mathcal{O}(1/V)$ terms vanish in the limit $V\to\infty$ and $m_n'=m_n/V$ is the magnetization density. We thus find that the scarred states $|\mathcal{S}_n\rangle$ (aside from the zero-measure set with $m'=\pm 1$) possess spin-nematic ODLRO. This implies that the spin fluctuations in the x-y plane break the U(1) spin-rotation symmetry spontaneously without long-range magnetic order (i.e., time-reversal symmetry is preserved). This remarkable property also heralds ETH violation: ODLRO is impossible for ETH-obeying states in the middle of the spectrum [such states are nominally at infinite temperature, where the thermal density matrix $\rho=e^{-\beta H}$ in a given U(1) sector is trivial].

The ODLRO in Eq. (8) immediately implies that the scarred states also support long-range *space-time* correlations, the defining characteristic of space-time crystalline order [28,38]. Up to $1/V$ corrections, we have

$$\mathrm{Re}\langle\mathcal{S}_n|O_{\boldsymbol{\pi}}^\dagger(t)O_{\boldsymbol{\pi}}(0)|\mathcal{S}_n\rangle=(1-m_n'^2)\cos(2ht). \tag{9}$$

This space-time crystalline order can ultimately be traced back to the condensation of π bimagnons. We note that the existence of this order does not violate the no-go theorems establishing its impossibility at thermal equilibrium [28,39]; since the scarred states violate the ETH, these no-go theorems do not apply.

Dynamical signature of scars.—We now demonstrate that the eigenstate properties of $|\mathcal{S}_n\rangle$ derived above have significant consequences for the dynamics of local observables after certain quantum quenches. To illustrate, we initialize the system in the ground state $|\psi_0\rangle$ of the staggered rhombic anisotropy Hamiltonian

$$H_A = \frac{1}{2}\sum_i e^{i\mathbf{r}_i\cdot\boldsymbol{\pi}}[(S_i^x)^2 - (S_i^y)^2]. \tag{10}$$

This Hamiltonian is relevant to scarring since it can be rewritten in the form $H_A = \frac{1}{2}(J^+ + J^-) \equiv J^x$. $|\psi_0\rangle$ is thus the lowest-weight state of J_x in the spin-$V/2$ representation of the SU(2) algebra (4), which we call the "nematic Néel" state,

$$|\psi_0\rangle = \bigotimes_i \left(\frac{|m_i = +1\rangle - e^{i\mathbf{r}_i\cdot\boldsymbol{\pi}}|m_i = -1\rangle}{\sqrt{2}}\right). \tag{11}$$

Since this is an eigenstate of the spin-$V/2$ representation of Eq. (4), it resides entirely within the scarred manifold:

$$|\psi_0\rangle = \sum_{n=0}^{V} c_n|\mathcal{S}_n\rangle, \qquad c_n^2 = \frac{1}{2^V}\binom{V}{n}. \tag{12}$$

The fidelity of this initial state under evolution with H is thus given by

$$\mathcal{F}_0(t) = |\langle\psi_0|\psi_0(t)\rangle|^2 = \cos^{2V}(ht), \tag{13}$$

which exhibits perfect revivals with period $T = \pi/h$. As a result, all local observables oscillate with the revival period. This behavior is shown in Fig. 3, where we compare fidelities of other initial states that decay rapidly. The inset to Fig. 3 shows entanglement dynamics after a quench: while generic product states rapidly approach maximal entanglement, the special initial state $|\psi_0\rangle$ remains a product state under time evolution with H. Indeed, this evolution merely imparts phase factors $e^{\mp iht}$ to the terms $|m_i = \pm 1\rangle$ in Eq. (11). Physically this corresponds to a set of spin-nematic *directors* precessing in the x-y plane with frequency twice the applied field, see Fig. 4. The local director angle θ_i may be defined in terms of the phase of the local order parameter

$$O_i = (S_i^+)^2. \tag{14}$$

Time evolution yields $\langle\psi_0(t)|O_i|\psi_0(t)\rangle = e^{2iht} \equiv |O_i|e^{2i\theta_i}$ and hence the phase winds as $\theta_i = ht$ with $|O_i| = 1$. The directors thus oscillate coherently and in a synchronized fashion when initially staggered in space, as in Eq. (11) and shown schematically in Fig. 4.

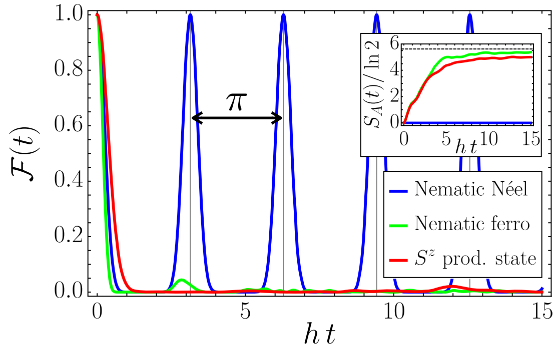

FIG. 3. Many-body fidelity $\mathcal{F}(t) = |\langle\psi(0)|\psi(t)\rangle|^2$ for various initial states ($d = 1$, $L = 8$, and remaining parameters as in Fig. 2). The nematic Néel initial state [Eq. (11)] exhibits perfect revivals described by Eq. (13), while generic initial states decay rapidly. (Inset) Entanglement dynamics after a quench, showing that generic initial states lead to rapid entanglement growth and saturation near the value for a random state (dashed line), while the special initial state does not.

Crucially, this dynamical behavior *does not* originate from a set of freely precessing directors. If it did, the "nematic ferro" state (with directors aligned) would also show oscillations, and this is clearly not the case (cf. Fig. 3). Rather, the observed revivals originate from the precession of a single emergent *macroscopic* staggered director. The existence of this director is enabled by the long-range connected correlations in the scarred states $|\mathcal{S}_n\rangle$, which in turn originate from the emergent SU(2) algebra (4).

Finally, we note that the scarred states persist in the presence of the staggered rhombic anisotropy H_A, Eq. (10). Because $H_A \propto J^x$, it cants the effective magnetic field about which the macroscopic director precesses (indeed, more generally, one can add an additional anisotropy $H_B \propto J^y$). The resulting scarred eigenstates can be obtained from the states $|\mathcal{S}_n\rangle$ by an appropriate SU(2) rotation using the generators (4). This observation implies that one need not quench the staggered anisotropy in order to observe persistent oscillations. In a system with *fixed* staggered

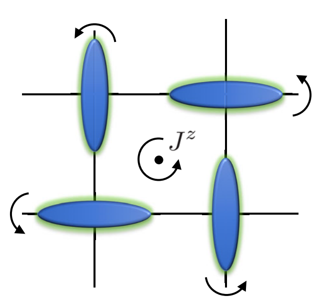

FIG. 4. Schematic of the spin-nematic order parameter on a 2D square lattice precessing around the applied field, $\sum_i S_i^z \propto J^z$. The staggered local directors (blue ovals) are synchronized such that their dynamics stay within the manifold of scarred states, cf. Eqs. (12)–(14).

rhombic anisotropy as in Eq. (10), one may instead polarize the initial state by applying a large homogeneous magnetic field $\propto J^z$. The dynamics of the fully polarized state will then show persistent oscillations due to the presence of the rotated scarred states, whereas generic states will not.

Conclusion.—In this Letter, we uncovered a set of exact scarred eigenstates in nonintegrable spin-1 XY magnets, leading to weak ergodicity breaking and strong-ETH violation. These states have properties that are impossible in ETH-obeying states, including subextensive entanglement entropy and spin-nematic ODLRO. The scarred states are maximal-spin eigenstates of an emergent SU(2) algebra that does not commute with the Hamiltonian. Using this algebra, we showed that the scarred states enable coherent many-body revivals following suitable quantum quenches.

This Letter provides a novel context in which several hypothesized characteristics of QMBS in the Rydberg-atom quantum simulator [20] become exact. For example, in Ref. [14] it was suggested that an emergent SU(2) algebra could be responsible for the observed revivals, while Ref. [19] numerically demonstrated ODLRO and space-time crystalline order in the scarred states. Thus, the exact scarred states uncovered here suggest a common paradigm for QMBS that could be relevant across various physical models and which can be compared with other exact mechanisms leading to strong-ETH violation, including embedded Hilbert spaces [18,21,24,30] and emergent invariant subspaces [8,9,40]. This Letter also opens the possibility of searching experimentally for scarred dynamics in physical XY magnets with appropriate single-ion anisotropies or engineering it in superconducting circuits that could simulate spin-1 XY models.

We thank C.-J. Lin for pointing out the connection between our results and those of Ref. [24], on which we comment further in the Supplemental Material [30]. This work is supported by Microsoft and the Laboratory for Physical Sciences. T. I. acknowledges a JQI postdoctoral fellowship and Iowa State University startup funds.

[1] J. M. Deutsch, Phys. Rev. A **43**, 2046 (1991).
[2] M. Srednicki, Phys. Rev. E **50**, 888 (1994).
[3] L. D'Alessio, Y. Kafri, A. Polkovnikov, and M. Rigol, Adv. Phys. **65**, 239 (2016).
[4] J. M. Deutsch, Rep. Prog. Phys. **81**, 082001 (2018).
[5] D. A. Abanin, E. Altman, I. Bloch, and M. Serbyn, Rev. Mod. Phys. **91**, 021001 (2019).
[6] P. Calabrese, F. H. L. Essler, and G. Mussardo, J. Stat. Mech. (2016) 064001.
[7] S. Pai and M. Pretko, arXiv:1903.06173 [Phys. Rev. Lett. (to be published)].
[8] V. Khemani and R. Nandkishore, arXiv:1904.04815.
[9] P. Sala, T. Rakovszky, R. Verresen, M. Knap, and F. Pollmann, arXiv:1904.04266.
[10] S. Moudgalya, S. Rachel, B. A. Bernevig, and N. Regnault, Phys. Rev. B **98**, 235155 (2018).
[11] C. J. Turner, A. A. Michailidis, D. A. Abanin, M. Serbyn, and Z. Papić, Nat. Phys. **14**, 745 (2018).
[12] C. J. Turner, A. A. Michailidis, D. A. Abanin, M. Serbyn, and Z. Papić, Phys. Rev. B **98**, 155134 (2018).
[13] S. Moudgalya, N. Regnault, and B. A. Bernevig, Phys. Rev. B **98**, 235156 (2018).
[14] S. Choi, C. J. Turner, H. Pichler, W. W. Ho, A. A. Michailidis, Z. Papić, M. Serbyn, M. D. Lukin, and D. A. Abanin, Phys. Rev. Lett. **122**, 220603 (2019).
[15] V. Khemani, C. R. Laumann, and A. Chandran, Phys. Rev. B **99**, 161101(R) (2019).
[16] C.-J. Lin and O. I. Motrunich, Phys. Rev. Lett. **122**, 173401 (2019).
[17] W. W. Ho, S. Choi, H. Pichler, and M. D. Lukin, Phys. Rev. Lett. **122**, 040603 (2019).
[18] S. Ok, K. Choo, C. Mudry, C. Castelnovo, C. Chamon, and T. Neupert, arXiv:1901.01260.
[19] T. Iadecola, M. Schecter, and S. Xu, arXiv:1903.10517.
[20] H. Bernien, S. Schwartz, A. Keesling, H. Levine, A. Omran, H. Pichler, S. Choi, A. S. Zibrov, M. Endres, M. Greiner *et al.*, Nature (London) **551**, 579 (2017).
[21] N. Shiraishi, J. Stat. Mech. (2019) 083103.
[22] A. A. Michailidis, C. J. Turner, Z. Papić, D. A. Abanin, and M. Serbyn, arXiv:1905.08564.
[23] S. Moudgalya, B. A. Bernevig, and N. Regnault, arXiv:1906.05292.
[24] N. Shiraishi and T. Mori, Phys. Rev. Lett. **119**, 030601 (2017).
[25] F. M. Surace, P. P. Mazza, G. Giudici, A. Lerose, A. Gambassi, and M. Dalmonte, arXiv:1902.09551.
[26] I. Affleck, T. Kennedy, E. H. Lieb, and H. Tasaki, Phys. Rev. Lett. **59**, 799 (1987).
[27] F. Wilczek, Phys. Rev. Lett. **109**, 160401 (2012).
[28] H. Watanabe and M. Oshikawa, Phys. Rev. Lett. **114**, 251603 (2015).
[29] K. Sacha and J. Zakrzewski, Rep. Prog. Phys. **81**, 016401 (2017).
[30] See Supplemental Material at http://link.aps.org/supplemental/10.1103/PhysRevLett.123.147201 for derivations of the scarred eigenstates, an exact calculation of the entanglement spectrum for the states $|\mathcal{S}_n\rangle$ and the asymptotics of the entanglement entropy, discussion of the relationship to embedded Hamiltonians, and generalizations of the states $|\mathcal{S}_n\rangle$ to arbitrary spin S.
[31] A. Kitazawa, K. Hijii, and K. Nomura, J. Phys. A **36**, L351 (2003).
[32] A. Pal and D. A. Huse, Phys. Rev. B **82**, 174411 (2010).
[33] G. Biroli, C. Kollath, and A. M. Läuchli, Phys. Rev. Lett. **105**, 250401 (2010).
[34] D. N. Page, Phys. Rev. Lett. **71**, 1291 (1993).
[35] C. N. Yang, Phys. Rev. Lett. **63**, 2144 (1989).
[36] O. Vafek, N. Regnault, and B. A. Bernevig, SciPost Phys. **3**, 043 (2017).
[37] C. N. Yang, Rev. Mod. Phys. **34**, 694 (1962).
[38] V. Khemani, C. W. von Keyserlingk, and S. L. Sondhi, Phys. Rev. B **96**, 115127 (2017).
[39] P. Bruno, Phys. Rev. Lett. **111**, 070402 (2013).
[40] T. Iadecola and M. Žnidarič, Phys. Rev. Lett. **123**, 036403 (2019).